

PAPER • OPEN ACCESS

Time mirror in a lumped transmission line

To cite this article: Tom A Kuusela 2025 *Eur. J. Phys.* **46** 045204

View the [article online](#) for updates and enhancements.

You may also like

- [Retraction Notice: Direct Upcycling Spent LiFePO₄ Cathode Material by Pre-Oxidation and Al-V Co-Doping Strategy](#)
- [Determination of the Abundance of Mercury from the Hg II Line at 5677.10 Å. XXIII. HD 90264 B \(L Car\)](#)
Richard Monier
- [3I/ATLAS is Smaller or Rarer than It Looks](#)
Abraham Loeb

Time mirror in a lumped transmission line

Tom A Kuusela 

Department of Physics and Astronomy, University of Turku, 20014 Turku, Finland

E-mail: tom.kuusela@utu.fi

Received 8 January 2025, revised 26 May 2025

Accepted for publication 12 June 2025

Published 2 July 2025



CrossMark

Abstract

Refraction and reflection of wave motion are fundamental phenomena studied across various physics domains. These effects occur when waves encounter spatial changes in the medium, such as obstacles or variations in refractive index. Traditionally, these boundaries are spatially localized but persist over time. The linear wave equation, symmetric in space and time, suggests the possibility of a temporal counterpart to spatial mirrors. A temporal mirror, unlike a spatial one, is spatially extended but temporally confined to brief instances. This can be realized by abruptly altering the medium's properties within a timescale shorter than the wave's dynamics. This study presents a temporal mirror implemented in a one-dimensional electrical transmission line. Numerical simulations were conducted to understand the system's behavior and study system dynamics in more details. Numerical and experimental results confirmed that the temporal mirror effectively converges the wave towards its original shape, validating theoretical predictions.

Supplementary material for this article is available [online](#)

Keywords: wave equation, temporal mirror, transmission line, Green's function

1. Introduction

Refraction and reflection of wave motion are essential and widely studied phenomena in various areas of physics. Such phenomena are possible when a wave encounters spatial changes in the medium, such as obstacles, changes in the refractive index, or other



Original content from this work may be used under the terms of the [Creative Commons Attribution 4.0 licence](#). Any further distribution of this work must maintain attribution to the author(s) and the title of the work, journal citation and DOI.

inhomogeneities, generally referred to as spatial boundaries. These boundaries are spatially localized but temporally delocalized, as they are constantly present. The linear wave equation, which can model the dynamics of waves in many physical systems, is mathematically symmetric with respect to the exchange of time and space. Therefore, it is natural to seek a temporal counterpart to a spatial mirror. Such a temporal mirror, unlike a spatial mirror, is spatially delocalized because it exists throughout the dynamic space of the system, but temporally localized because it typically exists only for a brief moment. In practice, a temporal mirror can be implemented by abruptly changing the properties of the medium uniformly. For the mirror to function effectively, the properties of the medium must be changed on a timescale shorter than the dynamics of the propagating wave. This requirement significantly complicates the exploitation of the phenomenon, especially in optics. Temporal refraction has been experimentally verified in various systems such as photonic crystals [1], light control in metamaterials [2] and temporal control of graphene plasmons [3]. So far, a temporal mirror has only been successfully implemented in classical water waves [4, 5], in a transmission line made with microwave-range metamaterials [6] and recently in a quantum mechanical lattice formed by ultracold atoms [7].

Particularly in the case of the temporal mirror, the reflected wave has an interesting property: time appears reversed for it, which is why such a mirror is also called a 'time mirror'. In reality, the flow of time does not actually reverse—that is, the signal does not travel into the past—but rather, the signal propagates forward in time and backward in space, while its characteristics change as if time had been reversed. Practically, this means that in a dispersive system, the inevitable spreading of the wave as it propagates now reverses, and the wave begins to converge towards its original shape as it progresses. This opens up new possibilities for wave control.

The dispersion and other distortions of waves have long been compensable with a technique where the wavefront is measured from multiple points by some detectors, and based on this, new waves are calculated and transmitted back with suitable actuators or emitters to make the wave converge towards the desired shape [8–11]. This approach, known as time-reversal mirrors (TRMs), is based on the fact that any wave field within a given volume is fully determined by the wave field on the surface enclosing that volume. The method is different from a time mirror, but they also share some common features [12]. The TRM technique typically requires a lot of energy and processing power, and thus a temporal mirror could be a more efficient solution.

In this work, we present a temporal mirror implemented in a lumped electrical transmission line. The system is one-dimensional and thus quite easy to construct and measure in practice. The frequency band of the transmission line can be chosen to be quite low with suitable component choices, which facilitates experimental analysis of the transmission line. Since a real transmission line always contains imperfections, the most significant of which is dissipation, we first present numerical simulations of the transmission line, making it easier to see how this system works and how well it corresponds to mathematical predictions.

As a mathematical model, we use the simplest linear wave equation, whose solutions are quite familiar to most students from many other contexts in physics studies. However, in the case of the temporal mirror, solving the wave equation is more complex. We show first the basic properties of the solution using only elementary mathematical steps. The more general method based on Green's functions is explained in [Appendix](#).

2. Time mirror in wave equation

The one-dimensional homogeneous wave equation can be written in the form

$$c^2 \frac{\partial^2 \psi(x, t)}{\partial x^2} - \frac{\partial^2 \psi(x, t)}{\partial t^2} = 0. \quad (1)$$

If the initial conditions $\psi(x, 0) = \phi(x)$ and $\partial\psi(x, 0)/\partial t = \theta(x)$ are known, the solution can be written in the well-known form [13]

$$\psi(x, t) = \frac{1}{2}[\phi(x - ct) + \phi(x + ct)] + \frac{1}{2c} \int_{x-ct}^{x+ct} \theta(s) ds. \quad (2)$$

If, for example, $\theta(x) = 0$, we obtain a solution that consists of two identical parts travelling in opposite directions. The similar situation occurs when $\phi(x) = 0$.

The temporal mirror (also called instantaneous time mirror or ITM [4]) can be realized by introducing a sudden change in the properties of the wave medium. In practice, this disruption can be modelled by a Dirac's δ -function such that the wave velocity has the time dependence

$$c^2(t) = c_0^2[1 + \gamma\delta(t - t_0)], \quad (3)$$

where t_0 is the time moment of this temporally localized but spatially non-localized disruption and the parameter γ is the strength of this effect. By substituting the term $c^2(t)$ into equation (1) we obtain

$$\frac{\partial^2 \psi(x, t)}{\partial x^2} - \frac{1}{c_0^2} \frac{\partial^2 \psi(x, t)}{\partial t^2} = -\gamma\delta(t - t_0) \frac{\partial^2 \psi(x, t)}{\partial x^2}. \quad (4)$$

For all other times than t_0 , the Dirac's function has no role and equation (4) is still an usual homogeneous wave equation. Therefore, we can calculate the right-hand side of equation (4) at the time moment of t_0 . Since for all times prior to t_0 , $\psi(x, t)$ is the solution of equation (1), we can replace $\frac{\partial^2 \psi(x, t)}{\partial x^2}$ with $\frac{1}{c_0^2} \frac{\partial^2 \psi(x, t)}{\partial t^2}$. Finally, we have

$$\left(\frac{\partial^2 \psi(x, t)}{\partial x^2} \right) - \frac{1}{c_0^2} \frac{\partial^2 \psi(x, t)}{\partial t^2} = -\frac{\gamma}{c_0^2} \delta(t - t_0) \frac{\partial^2 \psi(x, t_0)}{\partial t^2}. \quad (5)$$

Next, we can imagine that the system is 'frozen' at the moment of the temporal mirror. Just before the mirror, the wave solution is solely determined by the initial condition ($\psi(x, t_0)$, $\partial\psi(x, t_0)/\partial t$), and this part of the solution continues unchanged after the temporal mirror. At $t = t_0$, the effect of the term on the right-hand side of equation (5) can be interpreted as an additional initial condition (0 , $\gamma\partial^2\psi(x, t_0)/\partial t^2$) (for the mathematical proof, see Appendix). According to equation (2), this initial condition generates the solution

$$\theta_{fw}(x, t) - \theta_{bw}(x, t) = \frac{\gamma}{2} \frac{\partial\psi(x, t)}{\partial t} - \frac{\gamma}{2} \frac{\partial\psi(x, -t)}{\partial t}, \quad (6)$$

i.e. two new waves travelling in opposite directions for $t > t_0$, as shown schematically in figure 1.

The solutions of the wave equations (1) or (5) are non-dispersive, i.e. all frequency components of the solution travel at equal velocity. In other words, the phase velocity of these components does not depend on the frequency. However, it can be shown that also in the case of dispersive system, we have those three wave fields but especially the θ_{fw} and θ_{bw} have more complex mathematical form [4].

Although the wave fields $\theta_{fw}(x, t)$ and $\theta_{bw}(x, t)$ are proportional to the time derivative of the original wave, they can be also quite closely proportional to the original wave itself (excluding the phase shift) if the bandwidth of the wave is not too large. In that case, the time-

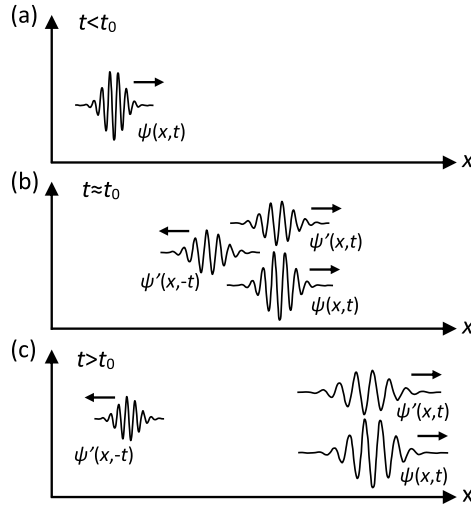


Figure 1. Schematic of the solutions of the wave equation with a temporal mirror. The system is assumed to be dispersive. (a) The initial wave pulse propagates to the right. (b) At the temporal mirror event, the original wave continues unchanged, while two new waves propagating in opposite directions are generated ($\psi'(x, t) = \frac{\partial \psi(x, t)}{\partial t}$). (c) Due to the dispersion, the waves propagating to the right gradually spread, while the one propagating to the left narrows, thereby compensating the effect of the dispersion.

reversed wave θ_{bw} is highly interesting as it can eliminate the effect of dispersion when travelling backwards: the wave converges towards the original shape as we will see in numerical and partially also in experimental results (see also figure 1).

3. Lumped transmission line

The schematics of the lumped transmission line is shown in figure 2. The circuit equations are

$$L \frac{di_n}{dt} = v_{n-1} - v_n, \quad (7)$$

$$C \frac{dv_n}{dt} = i_n - i_{n+1}, \quad (8)$$

where $i_n(t)$ is the current, $v_n(t)$ the voltage, L the inductance and C the capacitance. No dissipative effects have been taken into account here. We assume that the transmission line is infinite. By differentiating both sides of equation (8) respect to the time and using equation (7), we get the differential-difference equation for the voltage

$$\frac{d^2 v_n}{dt^2} = \frac{1}{LC} (2v_n - v_{n-1} - v_{n+1}). \quad (9)$$

In the long-wave limit, we can assume that the index n is a continuous variable, and thus we can approximate $v_n - v_{n-1} \approx \partial v(n, t) / \partial n$. In this limit, we obtain the differential equation (we replace n with x)

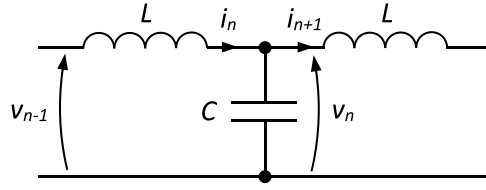


Figure 2. One section of the electrical transmission line.

$$\frac{\partial^2 v(x, t)}{\partial t^2} = \frac{1}{LC} \frac{\partial^2 v(x, t)}{\partial x^2}. \quad (10)$$

This is a homogeneous wave equation which supports wave propagation at the velocity of $1/\sqrt{LC}$ without any dispersion, and therefore the solution can be given by equation (2). However, if we search the solution of the original equation (9) in the form of $v_n(t) = Ae^{i(kn-\omega t)}$, we get the dispersion relation

$$\omega^2 = \omega_0^2 \sin^2(k/2), \quad \omega_0 = \frac{2}{\sqrt{LC}}. \quad (11)$$

Clearly, the phase velocity $v_p = \omega/k$ is not constant and the system is dispersive except in the long-wave limit $k \ll 1$.

4. Experimental setup

One section of the experimental transmission line is shown in figure 3. The inductance L (EPCOS B82144A2105J000) is 1 mH with the serial resistance of 2.8Ω . The serial resistance should be as small as possible since it directly affects on the dissipation of the system. In practice, a real inductor is not a series connection of an ideal inductance and a pure resistance, but its losses also depend on frequency in a complex way. Therefore, accurate modelling—for example, numerically—is challenging. The total capacitance of each section consists of two capacitors C_1 (1 nF) and C_2 (10 nF) connected in parallel. With these values, the wave velocity is approx. 0.3 lattice site/ μ s.

The temporal mirror is realized by changing simultaneously and abruptly the capacitance of all sections. This is done with the MOSFET switch T_1 (BS170). Normally, the gate voltage of T_1 is high (4.5 V), the transistor is in the on-mode and the capacitance C_2 is a part of the system. During the time mirror, the gate voltage is dropped down for a short moment of time (4 μ s), T_1 goes to the off-mode and C_1 is disconnected. It should be emphasized that this kind of circuit arrangement is not exactly the same as just changing the value of the capacitance since the charge of C_2 is isolated from the rest of the circuit during the off-period of the transistor. In ideal system, as in our numerical simulations, this charge does not disappear from the system but it affects on the system dynamics all the time. However, as we will see later, this circuit system can mimic the temporal mirror surprisingly well.

The total number of the sections is 47. Whole circuitry is built into a prototype breadboard which does not need any soldering, thus components can be easily changed. The transmission line should be constructed in a shape of straight line since it is sensitive to all turns and other structural inhomogeneities which produce signal reflections and noise background. The line should be terminated with a resistance of the transmission line's characteristic impedance $Z = \sqrt{L/C}$ (here approx. 300Ω) in order to avoid a pulse reflection.

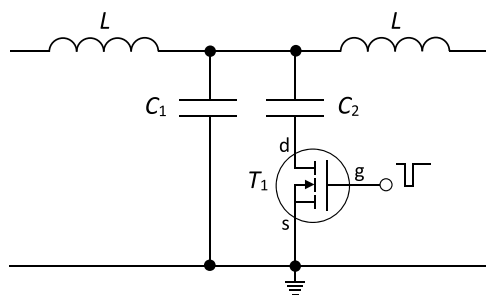


Figure 3. Experimental realization of the lumped electrical transmission line with the temporal mirror. The MOSFET T_1 switches produce an abrupt change in the capacitance of all lattice sites.

The travelling wave is created by feeding a short pulse (amplitude 2 V, length 15 μs) into the beginning of the transmission line. One pulse generator is used for the input pulse and another one triggered by the first one to create the control pulse for all MOSFETs.

Studying the behavior of the temporal mirror becomes easier if the state of the transmission line is represented as a function of the lattice site. This can be done as follows. The voltage signal is collected from all lattice sites as a function of time using computer controlled oscilloscope (the sampling rate 4 Ms s^{-1}). One channel of the oscilloscope is used to measure the the input pulse and trigger the data collection. The other channel is used to collect data from all lattice sites, one by one. This arrangement ensures that all collected signals have a common time line. The time series data from each lattice site is imported into the spread sheet program as a column. When the time series has been measured at each lattice site, we obtain a fairly large matrix, where the columns correspond to the lattice site variable and the rows represent increasing time instants. Finally, by picking one row from the complete data set we get the content of the transmission line as a function of the lattice site at a certain moment of time.

5. Numerical results

Simulations are performed by numerical integration of the circuit equations (7) and (8). The dynamical variables are scaled in the manner that $L = C = 1$. We use the fourth-order Runge–Kutta algorithm in numerical integration, the time step is 2×10^{-5} and the number of lattice sites 100. In the initial state, all currents and voltages are zero, and the voltage of the first section is set to be 1 during the time interval of 1. The time mirror is generated by changing the value of C from 1 to 15 over the time interval of 2.

The time evolution of the input pulse without the temporal mirror is shown in figure 4 (left panel). We can clearly see that the input pulse is gradually broadening and oscillations are creating behind the main pulse due to the dispersion. When the temporal mirror is switch on at $t = 50$ (figure 4, right panel), the original wave is propagating almost unperturbed but the reflected wave is created. As this wave propagates, it finally converges towards the shape which is very similar as the original input pulse (see also the videos in Supplementary materials).

In order to check if there really exist those three different wave fields after the temporal mirror as described in Chapter II, we present few snapshots in figure 5. By subtracting the signal without the temporal mirror at the time moment of $t = 95$ [figure 5(a)] from the the

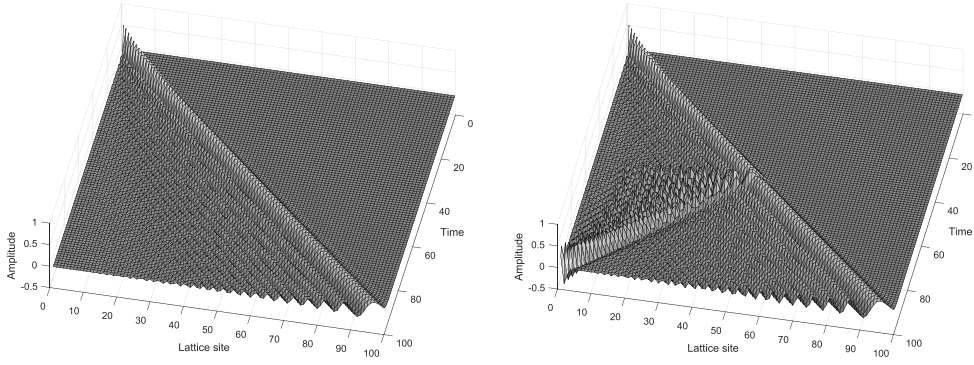


Figure 4. Time evolution of the input pulse without the temporal mirror (left panel) and with the temporal mirror (right panel) at the time moment $t = 50$.

signal after the temporal mirror at the same time moment [figure 5(b)], we have the signal in figure 5(c). The signal in figure 5(d) is the time derivative of the signal in figure 5(a). When we compare the signals in figures 5(c) and (d) in the lattice range of 70–100, we found that they are very similar except a minor difference in the amplitude scale. Thus we can conclude that the temporal mirror signal really consists of the original unperturbed wave field and its time derivative signal propagating in the same direction.

In figure 6 we study the reflecting part of the wave field. The signal after the temporal mirror at $t = 120$ is shown in figure 6(b), and the reflected pulse is clearly visible. Since at this moment of time the signal without the temporal mirror is almost zero in the lattice range of 0–20, there is no need to subtract it for comparisons. In figure 6(c) we have integrated the system for so long ($t = 21.9$) that the maximum derivative of the signal [figure 6(d)] is in exactly the same place as the pulse maximum in figure 6(b). By comparing the temporal mirror signal and the derivative signal in the lattice range of 0–20, we find that they are almost identical, and the reflecting pulse is the time reversed version of the forward propagating derivative wave.

The temporal mirror is thus capable of generating two other waves in addition to the original wave. Since waves are always associated with momentum and energy, it is interesting to study how they can change. It can be shown that an temporal discontinuity in a homogeneous medium conserves the momentum but not the energy [4, 5, 14]. In our transmission line system the total energy is the sum of energy in the inductors and capacitors

$$E_{\text{tot}} = \frac{1}{2}L \sum_n i_n^2 + \frac{1}{2}C \sum_n v_n^2. \quad (12)$$

The total energy as a function of time is shown in figure 7. After the input pulse has fed energy into the system, the energy is constant but it abruptly jumps up after the temporal mirror: the temporal mirror has increased system's total energy.

6. Experimental results

Experimental time evolution of the signal in the transmission line is presented in figure 8. When we have no temporal mirror (left panel), the voltage pulse travels with almost constant velocity. The pulse spreads because of the dispersion, and the amplitude decreases due to the dissipation. We can see some oscillatory tail but not strong one. With the temporal mirror, the

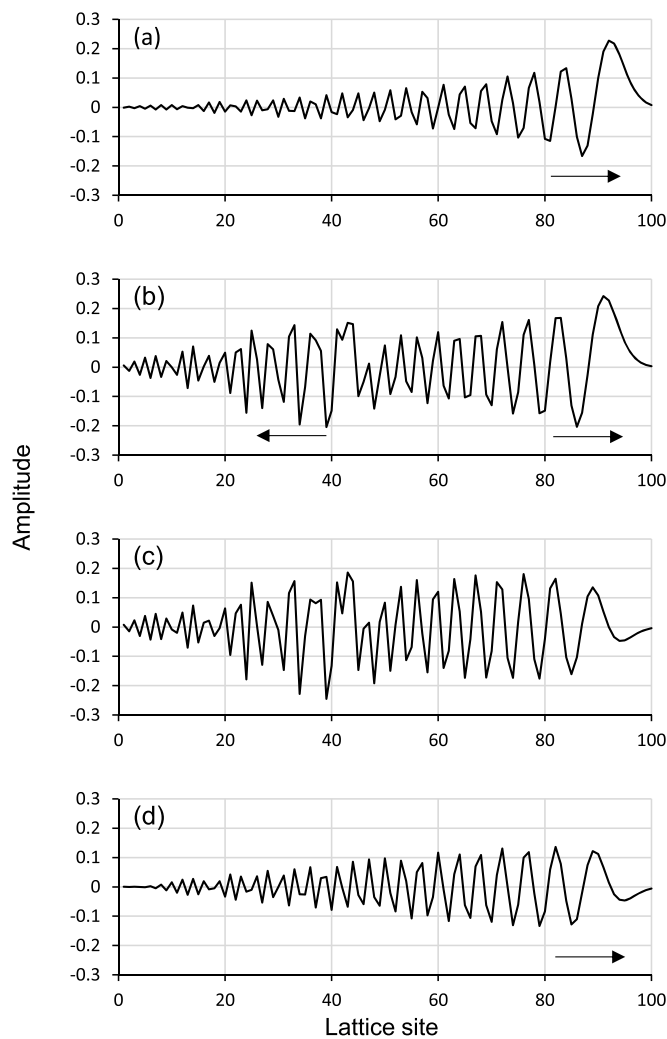


Figure 5. The amplitude of the numerical signal as a function of the lattice site. (a) The signal at $t = 95$ without the temporal mirror. (b) The signal at $t = 95$ with the temporal mirror at $t = 70$. (c) The difference (b)–(a). (d) The time derivative of the signal (a).

reflecting wave is generated (right panel). The amplitude of the reflecting wave is not actually decreasing since obviously the wave convergence due to time reversal at least partially compensates damping produced by dissipation.

Some snapshots of the wave propagation are shown in figure 9. When the signal without the temporal mirror is subtracted from the one with the temporal mirror, we get the signal in figure 9(c). The result consists of two opposite direction propagating pulses whose shapes resemble the derivative of the unperturbed wave. We can therefore state that at least qualitatively the dynamics of the transmission line with the temporal mirror follow the theoretical prediction, even under significant dissipation. The experimental results cannot be directly compared with the numerical ones, not even if we account for a simple dissipative mechanism, because the losses in the inductor behave in a complex manner and the implementation of the temporal mirror is different. It should be also noted that the temporal mirror circuitry used in this

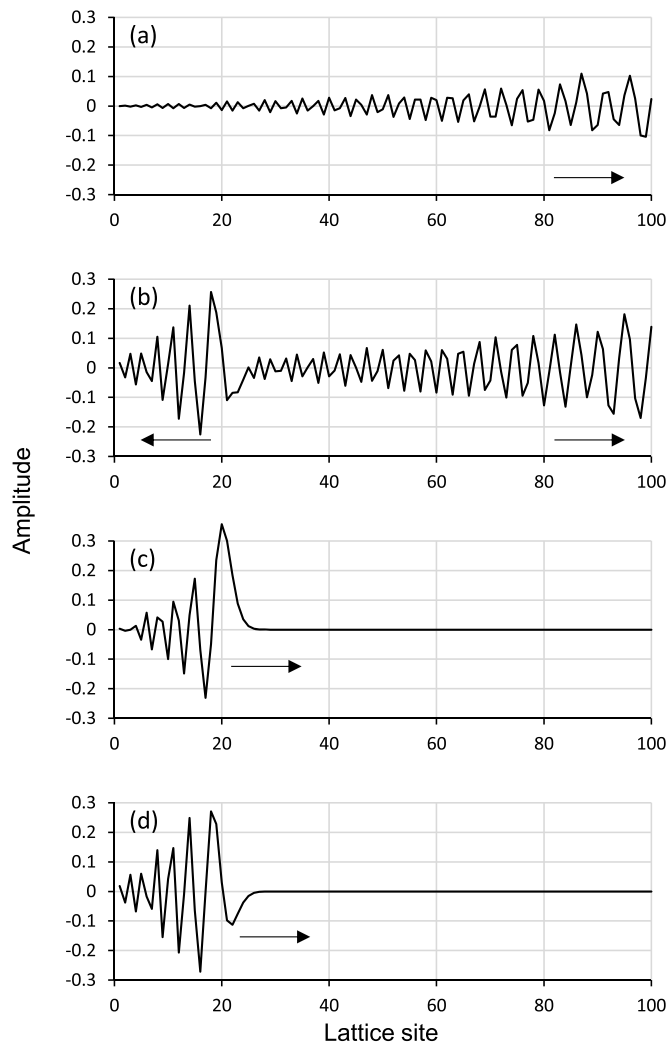


Figure 6. The amplitude of the numerical signal as a function of the lattice site. (a) The signal at $t = 120$ without the temporal mirror. (b) The signal at $t = 120$ with the temporal mirror at $t = 70$. (c) The signal at $t = 21.9$ without the time mirror. (d) The time derivative of the signal (c).

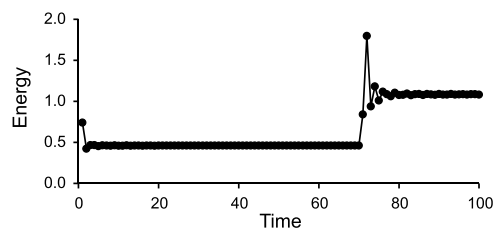


Figure 7. The total energy of the transmission line as a function of time. The temporal mirror takes place at $T = 70$.

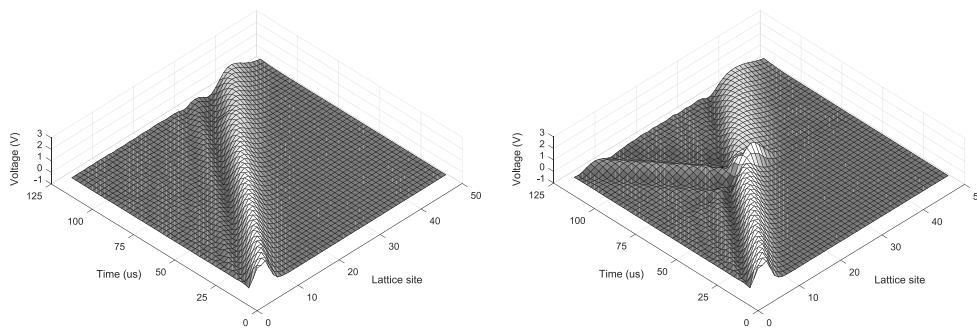


Figure 8. Experimental time evolution of the input pulse without the temporal mirror (left panel) and with the temporal mirror (right panel) at the time moment $t = 65 \mu\text{s}$.

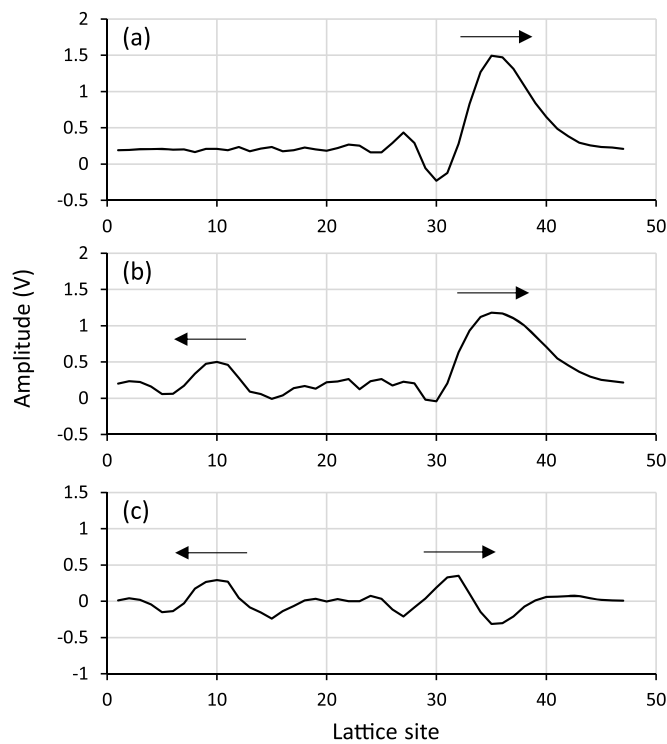


Figure 9. The amplitude of the experimental signal as a function of the lattice site. (a) The signal at $t = 115 \mu\text{s}$ without the temporal mirror. (b) The signal at $t = 115 \mu\text{s}$ with the temporal mirror at $t = 65 \mu\text{s}$. (c) The difference (b)–(a).

experimental setup does not feed any energy into this system [15], as a contrast to numerical simulations, and the time reversal does not compensate dissipation, only dispersion.

7. Concluding remarks

For physics students, the linear wave equation is generally very familiar, and its solution can be easily found with a suitable trial function. The wave equation also has numerous

applications in several key areas of physics, such as mechanics, acoustics, and optics. On the other hand, the symmetry between time and space in the wave equation, as obvious as it is, usually does not attract any particular attention or inspire new physical phenomena related to it. The temporal mirror challenges students to think about this simple system from a new perspective.

Analytical treatment of the time mirror requires more advanced mathematical skills and naturally leads to a general solution method based on Green's functions. Since Green's functions are widely used in various fields of physics, it is well justified for students to become familiar with them. Therefore we show the detailed calculations in [Appendix](#). However, the basic properties of the temporal mirror in the wave equation can be understood without any knowledge of Green's functions.

The discrete transmission line as an example system is easy to grasp, as the associated circuit equations are already familiar from basic electronics studies. Experimentally, the transmission line is also a good demonstration device because it is inexpensive to construct, and the measurements require only basic instruments found in most teaching laboratories. Numerical integration of the lumped transmission line is also easy because the spatial variable is inherently discrete, so it is not necessary to consider any numerical challenges of partial differential equations. A numerical simulation alone is also sufficient for studying the temporal mirror phenomenon if the experimental implementation is considered too cumbersome.

In physics research, temporal mirrors are a subject of active, albeit largely theoretical, interest, particularly in optics, where they introduce a new degree of freedom in controlling light, time. Time-reversal techniques and time-varying photonic media in general can offer totally new applications in all kind of wave control.

Data availability statement

All data that support the findings of this study are included within the article (and any supplementary files).

Appendix. General solutions of the wave equation

Let us first consider the general non-homogeneous three-dimensional wave equation

$$\nabla^2\psi(\mathbf{r}, t) - \frac{1}{c^2}\frac{\partial^2\psi(\mathbf{r}, t)}{\partial t^2} = \sigma(\mathbf{r}, t), \quad (\text{A}\cdot 1)$$

where ∇ is the gradient operator and c the velocity of the wave. Equation (1) can describe, for example, the transverse displacement of a vibrating string (one-dimensional version) or membrane (two-dimensional version) from equilibrium, when the source term $\sigma(\mathbf{r}, t)$ represents an external force. If the external force is of the harmonic form $\sigma(\mathbf{r}, t) = f(\mathbf{r})e^{-i\omega t}$, the solution is also of the form $\psi(\mathbf{r}, t) = \psi(\mathbf{r})e^{-i\omega t}$, meaning the equation is separable with respect to time and space. The spatial part of the solution is then obtained from the corresponding Helmholtz equation $(\nabla^2 + k^2)\psi(\mathbf{r}) = f(\mathbf{r})$, where $k = \omega/c$.

If the time dependence of the source function $\sigma(\mathbf{r}, t)$ is of a general form, we cannot, at least easily, separate the time and space dependence of the solution. For a general solution, we also need information about the initial conditions, meaning $\psi(\mathbf{r}, t)$ and $\partial\psi(\mathbf{r}, t)/\partial t$ are given at time $t = t_0$ throughout the volume V of the entire system. Additionally, it is usually necessary to define the boundary conditions, meaning the function $\psi(\mathbf{r}, t)$ itself and/or its normal derivative $\mathbf{n} \cdot \nabla \psi(\mathbf{r}, t)$ are specified on the surface S (\mathbf{n} is the surface normal). A general

method to solve the wave equation is based on Green's functions. It can be shown that the solution to equation (A-1) can be written in a general form that includes initial and boundary conditions [16, 17]

$$\begin{aligned} \psi(\mathbf{r}, t) = & \int_{t_0}^t dt' \int_V G(\mathbf{r}, t; \mathbf{r}', t') \sigma(\mathbf{r}', t') d\mathbf{r}' \\ & - \int_{t_0}^t dt' \oint_S d\mathbf{s} \cdot [G(\mathbf{r}, t; \mathbf{r}', t') \nabla \psi(\mathbf{r}', t') - \psi(\mathbf{r}', t') \nabla G(\mathbf{r}, t; \mathbf{r}', t')] \\ & - \frac{1}{c^2} \int_V d\mathbf{r}' \left[G(\mathbf{r}, t; \mathbf{r}', t') \frac{\partial \psi(\mathbf{r}', t')}{\partial t'} \Big|_{t'=t_0} \right. \\ & \left. - \psi(\mathbf{r}', t') \frac{\partial G(\mathbf{r}, t; \mathbf{r}', t')}{\partial t'} \Big|_{t'=t_0} \right], \end{aligned} \quad (\text{A-2})$$

where $G(\mathbf{r}, t; \mathbf{r}', t')$ is the so-called Green's function, S is the closing surface of the system volume V and $d\mathbf{s}$ is the outwardly directed surface element. The first integral in (A-2) represents the effect of the source $\sigma(\mathbf{r}, t)$, the second integral the boundary conditions, and the third one the effect of the initial conditions. The corresponding Green's function can be solved from the equation

$$\nabla^2 G(\mathbf{r}, t; \mathbf{r}', t') - \frac{1}{c^2} \frac{\partial^2 G(\mathbf{r}, t; \mathbf{r}', t')}{\partial t'^2} = \delta(\mathbf{r} - \mathbf{r}') \delta(t - t'), \quad (\text{A-3})$$

where $\delta(x)$ is the Dirac's delta-function. The functional form of $G(\mathbf{r}, t; \mathbf{r}', t')$ depends on the dimension of the system. In the case of one-dimensional system, we obtain

$$G(x, t; x', t') = \frac{1}{2c} H\left(t - t' - \frac{|x - x'|}{c}\right), \quad (\text{A-4})$$

where $H(x)$ is the Heaviside's step-function.

The solution of the specific wave equation (5) with the source term of the temporal mirror can be written by Green's function according to equation (A-2). We assume that the system has no boundaries, thus we can omit the second integral in equation (A-2), and we have contributions only from the source term and the initial conditions (we let $t_0 = 0$):

$$\begin{aligned} \psi(x, t) = & \int_0^t dt' \int dx' G(x, t; x', t') \left(-\frac{\gamma}{c_0^2}\right) \delta(t') \frac{\partial^2 \psi(x', t')}{\partial t'^2} \\ & - \frac{1}{c_0^2} \int dx' \left[G(x, t; x', 0) \frac{\partial \psi(x', 0)}{\partial t'} - \psi(x', 0) \frac{\partial G(x, t; x', 0)}{\partial t'} \right] \\ = & -\frac{1}{c_0^2} \int dx' G(x, t; x', 0) \frac{\partial}{\partial t'} \left[\gamma \frac{\partial \psi(x', 0)}{\partial t'} + \psi(x', 0) \right] \\ & - \frac{1}{c_0^2} \int dx' \psi(x', 0) \frac{\partial G(x, t; x', 0)}{\partial t'}. \end{aligned} \quad (\text{A-5})$$

Next we rewrite equation (A-5) by doing the following almost trivial substitutions

$$\gamma \frac{\partial \psi(x', 0)}{\partial t'} = \frac{\gamma}{2} \frac{\partial \psi(x', 0)}{\partial t'} + \frac{\gamma}{2} \frac{\partial \psi(x', 0)}{\partial t'}, \quad (\text{A-6})$$

$$\psi(x', 0) = \psi(x', 0) - \frac{\gamma}{2} \frac{\partial}{\partial t'} \psi(x', 0) + \frac{\gamma}{2} \frac{\partial}{\partial t'} \psi(x', 0). \quad (\text{A}\cdot 7)$$

By using equation (A.6) in the first integral and equation (A.7) in the second integral, we obtain

$$\begin{aligned} \psi(x, t) = & -\frac{1}{c_0^2} \int dx' G(x, t; x', 0) \frac{\partial}{\partial t'} \left[\psi(x', 0) + \frac{\gamma}{2} \frac{\partial}{\partial t'} \psi(x', 0) + \frac{\gamma}{2} \frac{\partial}{\partial t'} \psi(x', 0) \right] \\ & - \frac{1}{c_0^2} \int dx' \frac{\partial}{\partial t'} G(x, t; x', 0) \left[\psi(x', 0) + \frac{\gamma}{2} \frac{\partial}{\partial t'} \psi(x', 0) - \frac{\gamma}{2} \frac{\partial}{\partial t'} \psi(x', 0) \right]. \end{aligned} \quad (\text{A}\cdot 8)$$

We can see that the special source term originated from the temporal mirror behaves actually as an additional initial condition. In generally, assuming unbounded space, the solution of the wave equation for all times after the time moment of the mirror, here $t = 0$, is solely determined by the wave field itself (the terms in the brackets in the second integral) and its time derivative (the terms in the brackets in the first integral) everywhere in the space at the time moment $t = 0$. The first terms in the brackets in both integrals represent the original incident wave $\psi(x, t)$ travelling unperturbed after the time mirror. The second terms, respectively, represent another forward propagating wave field $\theta_{fw}(x, t) = \frac{\gamma}{2} \frac{\partial}{\partial t} \psi(x, t)$. The last terms in the brackets are similar but there is one extra minus sign. If we determine the new wave field $\theta_{bw}(x, t) = \frac{\gamma}{2} \frac{\partial}{\partial t} \psi(x, -t)$, we have $\theta_{bw}(x, 0) = \theta_{fw}(x, 0)$ and $\frac{\partial}{\partial t} \theta_{bw}(x, 0) = -\frac{\partial}{\partial t} \theta_{fw}(x, 0)$, thus there exists third time-reversed wave field.

ORCID iDs

Tom A Kuusela  <https://orcid.org/0000-0002-1436-9138>

References

- [1] Sharabi Y, Dikopoltsev A, Lustig E, Lumer Y and Segev M 2022 Spatiotemporal photonic crystals *Optica* **9** 585–92
- [2] Shaltout A M, Shalaev V M and Brongersma M L 2019 Spatiotemporal light control with active metasurfaces *Science* **364** eaat3100
- [3] Wilson J, Santosa F, Min M and Low T 2018 Temporal control of graphene plasmons *Phys. Rev. B* **98** 081411
- [4] Bacot V, Labousse M, Eddi A, Fink M and Fort E 2016 Time reversal and holography with spacetime transformations *Nat. Phys.* **12** 972–7
- [5] Peng D, Fan Y, Liu R, Guo X and Wang S 2020 Time-reversed water waves generated from an instantaneous time mirror *J. Phys. Commun.* **4** 105013
- [6] Moussa H, Xu G, Yin S, Galiffi E, Ra'di Y and Alù A 2023 Observation of temporal reflection and broadband frequency translation at photonic time-interfaces *Nat. Phys.* **19** 863–8
- [7] Dong Z, Li H, Wan T, Liang Q and Yang Z 2024 Quantum time reflection and refraction of ultracold atoms *Nat. Photon.* **18** 68–73
- [8] Fink M 1992 Time reversal of ultrasonic fields *IEEE Trans. Ultrason. Ferr. Freq. Control* **39** 555–66
- [9] Lerosey G, de Rosny J, Tourin A, Derode A, Montaldo G and Fink M 2004 Time reversal of electromagnetic waves *Phys. Rev. Lett.* **92** 193904
- [10] Draeger C and Fink M 1997 One-channel time reversal of elastic waves in a chaotic 2D-silicon cavity *Phys. Rev. Lett.* **79** 407–10
- [11] Prasadka A, Feat S and Petitjeans P 2012 Time reversal of water waves *Phys. Rev. Lett.* **109** 064501
- [12] Fink M and Fort E 2017 From the time-reversal mirror to the instantaneous time mirror *Eur. Phys. J. Special Topics* **226** 1477–86

-
- [13] Strauss W A 2008 *Partial differential equations* (Wiley)
- [14] In spatial reflection, some of the momentum of the wave is transferred to the mirror, i.e. it changes, but instead the energy is always retained: time-space symmetry is also visible here.
- [15] The gate circuit of the MOSFET is almost completely isolated from the actual transmission line, as there is only a very small capacitive coupling between the gate and the channel, through which the transferred energy is practically negligibl.
- [16] Copley L 2015 *Mathematics for the Physical Sciences* (De Gruyter Open)
- [17] Barton G 1989 *Elements of Green's Functions and Propagation: Potential, Diffusion, and Waves* (Oxford University Press)